

Multicolor lasing prints

Van Duong Ta, Shancheng Yang, Yue Wang, Yuan Gao, Tingchao He, Rui Chen, Hilmi Volkan Demir, and Handong Sun

Citation: *Applied Physics Letters* **107**, 221103 (2015); doi: 10.1063/1.4936628

View online: <http://dx.doi.org/10.1063/1.4936628>

View Table of Contents: <http://scitation.aip.org/content/aip/journal/apl/107/22?ver=pdfcov>

Published by the [AIP Publishing](#)

Articles you may be interested in

[Electro-pumped whispering gallery mode ZnO microlaser array](#)

Appl. Phys. Lett. **106**, 021111 (2015); 10.1063/1.4905925

[Random lasing from localized modes in strongly scattering systems consisting of macroporous titania monoliths infiltrated with dye solution](#)

Appl. Phys. Lett. **97**, 031118 (2010); 10.1063/1.3464962

[Simple largely tunable optical microcavity](#)

Appl. Phys. Lett. **89**, 081118 (2006); 10.1063/1.2335371

[Directional random lasing in dye- Ti O 2 doped polymer nanowire array embedded in porous alumina membrane](#)

Appl. Phys. Lett. **88**, 263112 (2006); 10.1063/1.2216853

[Phased-array electro-optic steering of large aperture laser beams using ferroelectrics](#)

Appl. Phys. Lett. **86**, 211113 (2005); 10.1063/1.1935033



MMR TECHNOLOGIES

**THE WORLD'S RESOURCE FOR
VARIABLE TEMPERATURE
SOLID STATE CHARACTERIZATION**

WWW.MMR-TECH.COM

OPTICAL STUDIES SYSTEMS SEEBECK STUDIES SYSTEMS MICROPROBE STATIONS HALL EFFECT STUDY SYSTEMS AND MAGNETS

Multicolor lasing prints

Van Duong Ta,^{1,a)} Shancheng Yang,^{1,a)} Yue Wang,¹ Yuan Gao,¹ Tingchao He,¹ Rui Chen,¹ Hilmi Volkan Demir,^{1,2,3,4} and Handong Sun^{1,4,b)}

¹*Division of Physics and Applied Physics, School of Physical and Mathematical Sciences, Nanyang Technological University, Singapore 637371, Singapore*

²*School of Electrical and Electronic Engineering, LUMINOUS! Center of Excellence for Semiconductor Lighting and Displays, Nanyang Technological University, Nanyang Avenue, Singapore 639798, Singapore*

³*Department of Electrical and Electronics Engineering and Department of Physics, UNAM–Institute of Materials Science and Nanotechnology, Bilkent University, Bilkent, Ankara TR-06800, Turkey*

⁴*Centre for Disruptive Photonic Technologies (CDPT), Nanyang Technological University, Singapore 637371, Singapore*

(Received 10 October 2015; accepted 16 November 2015; published online 30 November 2015)

This work demonstrates mass production of printable multi-color lasing microarrays based on uniform hemispherical microcavities on a distributed Bragg reflector using inkjet technique. By embedding two different organic dyes into these prints, optically pumped whispering gallery mode microlasers with lasing wavelengths in green and red spectral ranges are realized. The spectral line-width of the lasing modes is found as narrow as 0.11 nm. Interestingly, dual-color lasing emission in the ranges of 515–535 nm and 585–605 nm is simultaneously achieved by using two different dyes with certain ratios. Spectroscopic measurements elucidate the energy transfer process from the green dye (donor) to the red one (acceptor) with an energy transfer efficiency up to 80% in which the nonradiative Förster resonance energy transfer dominates. As such, the acceptor lasing in the presence of donor exhibits a significantly lower (~ 2.5 -fold) threshold compared with that of the pure acceptor lasing with the same concentration. © 2015 AIP Publishing LLC.

[<http://dx.doi.org/10.1063/1.4936628>]

Optical microcavities enhancing light-matter interactions by resonant recirculation are building blocks of cavity quantum electrodynamics, light sources, and active filters.¹ Microresonators with various geometries including Fabry-Perot, photonic crystal, distributed feedback, and whispering gallery mode (WGM) cavities have demonstrated a wide range of applications.^{2–5} Among these structures, WGM resonators have attracted increasing interests because of not only their promising applications such as ultra-sensitive biosensors,⁶ quantum devices,⁷ low-threshold and high quality (Q) factor microlasers^{8–10} but also their simple fabrication.^{11–13} Indeed, self-assembled droplets can serve as excellent WGM cavities and lasers based on droplet cavities have been realized and used for fast optical switches and gas sensors.^{14,15}

Recently, droplet cavities have been greatly benefited from the development of soft matter in optofluidics,¹⁶ microfluidics,¹⁷ and inkjet technique.^{18–20} The inkjet method is a cheap and powerful tool for mass production of droplet cavities with highly controlled cavity size and position.^{19,20} Investigation of inkjet method for fabricating high-Q microcavities, like hemispherical resonators,^{13,21} is an essential work because this approach opens opportunities to employ droplets for optical digital devices.^{22,23}

Lasers with selectable colors are in high demand for lighting and displays.^{24,25} In particular, multicolor lasers enabled by energy transfer, especially nonradiative Förster

resonance energy transfer (FRET),²⁶ are very interesting cases because they offer extended lasing wavelengths, high pumping efficiency, and low lasing threshold.^{27–29} In this work, high Q-factor, dual-color lasing from arrays of hemispherical microcavities fabricated by inkjet method is demonstrated.

The laser dyes used were Coumarin 540A (C540A, from Exciton) and Rhodamine B (RhB, from Sigma-Aldrich). C540A emits green light, which is well absorbed by RhB, and therefore, they make a good pair of donor (D) and acceptor (A), respectively. C540A (15.5 mg, 0.05 mmol) and RhB (24 mg, 0.05 mmol) were dissolved in dichloromethane (DCM, 0.15 mL, purity 99.76%) to make pure donor and acceptor solutions. To achieve multicolor lasing, the two dyes were mixed by adding separately 0.8, 1, 1.2, 1.6, 2.4, 4.9, and 24 mg RhB to individual pure C540A solutions, achieving mixtures with various D:A mole ratios of around 1:0.03, 1:0.04, 1:0.05, 1:0.07, 1:0.1, 1:0.2, and 1:1, respectively. Finally, the same amount (600 mg) of Araldite 506 (Sigma-Aldrich) was added into all of the solutions and thus ready for fabricating microcavities.

The hemispherical resonators are deposited on top of a distributed Bragg reflector (DBR) schematically shown in Fig. 1(a). This DBR has a stop-band width of about 140 nm, from 520 to 680 nm, with reflectivity up to 99.9% at 590 nm (Fig. 5(c)). The DBR is essential for achieving laser emission as it suppresses the optical loss leaking through the substrate.¹³

To get circular cavity structures, a thin layer of 1H,1H,2H,2H-perfluorooctyltriethoxysilane (a hydrophobic material) was coated on the DBR surface (Fig. 1(b)) before depositing droplets.²¹ Then, hemispherical resonators were

^{a)}V. D. Ta and S. Yang contributed equally to this work.

^{b)}Author to whom correspondence should be addressed. Electronic mail: hdsun@ntu.edu.sg

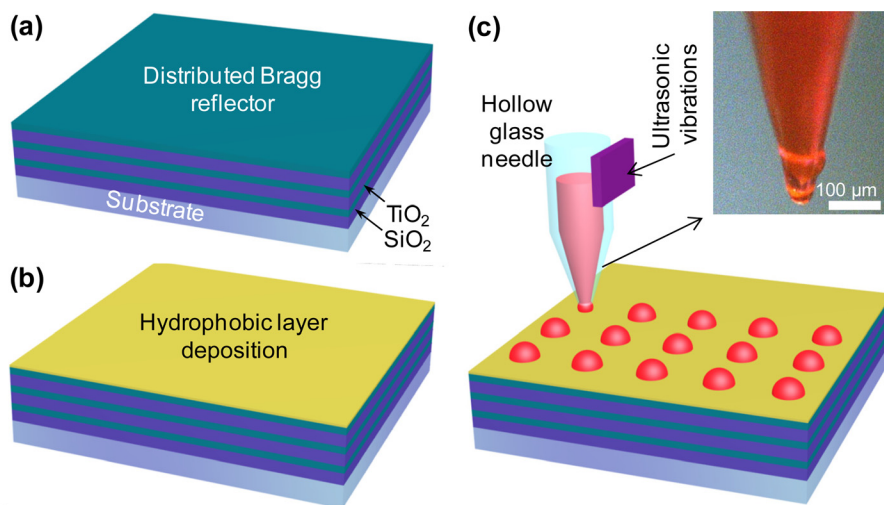


FIG. 1. (a) Schematic of the distributed Bragg reflector (DBR) substrate. (b) The deposition of a hydrophobic thin layer. (c) Fabrication principle of an array of hemispherical resonators on the hydrophobic DBR using a microplotter or inkjet technique.

fabricated using a GIXTM MicroplotterTM II from Sonoplot, INC (Fig. 1(c)). Figures 2(a) and 2(b) show arrays of uniform hemispheres formed using needles whose head diameters are about 30 and 80 μm , respectively. The cavity sizes rely on the glass needle used, which are about 35 and 85 μm . To examine the uniformity of the hemispheres, diameters of 173 hemispheres fabricated by the 30 μm needle were measured and their size distribution is plotted in Fig. 2(c). It can be seen that about 97% of the hemispheres have diameters $35 \pm 3 \mu\text{m}$ and approximately 56% have diameters $35 \pm 1 \mu\text{m}$. Furthermore, the distribution can be fairly fitted by a Gaussian curve.

Hemispheres were investigated using a microphotoluminescence ($\mu\text{-PL}$) setup. It consisted of a tunable Nd:YAG laser with a wavelength of 420 nm, pulse width of 5–6 ns and repetition rate of 20 Hz. The laser beam direction was $\sim 45^\circ$ normal to the DBR substrate, and the excitation spot has an elliptical shape with the dimension of $\sim 400 \times 500 \mu\text{m}$. Emission from the hemisphere was collected from the top side of the hemispheres by a microscope objective (50 \times , numerical aperture 0.42) and recorded by a silicon charge-coupled device (CCD) with a spectral resolution of around 0.06 nm.

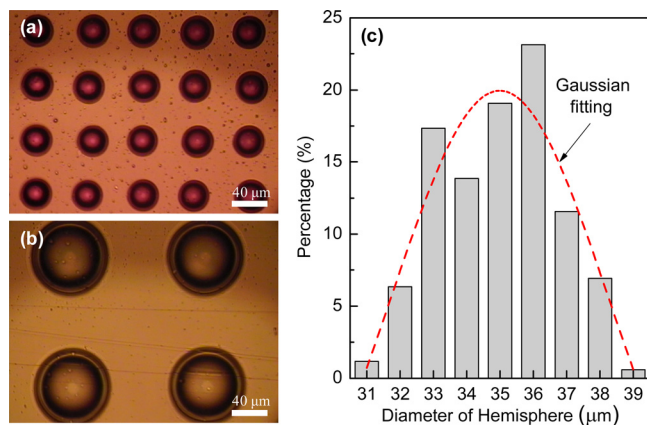


FIG. 2. (a) and (b) Optical images of regular arrays of hemisphere fabricated by a microplotter with 30 and 80 μm -diameters glass needles, respectively. The structures were doped with RhB (red) and C504A (green) dyes. (c) Diameter distribution of 173 hemispheres created using the 30 μm -diameter glass needle.

Laser emissions at green and red wavelengths upon optical pumping were observed from C540A and RhB separately doped hemispheres. Figure 3(a) shows the PL spectra from a $\sim 85 \mu\text{m}$ -diameter hemisphere with embedded C540A at pumping energy of about 3.0 and 7.3 μJ . At the low pumping energy, the spectrum was broad, and the intensity of the emission was weak. Therefore, the emission was dominated by spontaneous emission (SE). In contrast, sharp peaks with strong intensity, corresponding to lasing emission, appeared under higher excitation energy. Similarly, even though the absorption of the acceptor is relatively weak at 420 nm, the laser emission at red color (605 to 610 nm) was observed from a $\sim 57 \mu\text{m}$ -diameter RhB doped hemisphere (Fig. 3(b)). All lasing peaks were well separated with clear free spectral range (FSR) which supports a single cavity loop. Furthermore, due to the high refractive index contrast (0.41), the linewidth of the modes was about 0.11 nm, which is much narrower than 0.3 nm¹⁹ and $\sim 1 \text{ nm}$ ²⁰ reported previously where cavities fabricated by inkjet method from other materials.

The lasing mechanism is ascribed to WGMs and can be characterized by the radial (r) and angular (m) mode number. From the observation, there were no high order modes ($r > 1$) but a fundamental mode ($r = 1$). The mode number m can be simply expressed as $m = \pi n_c D / \lambda_m$, where λ_m is the

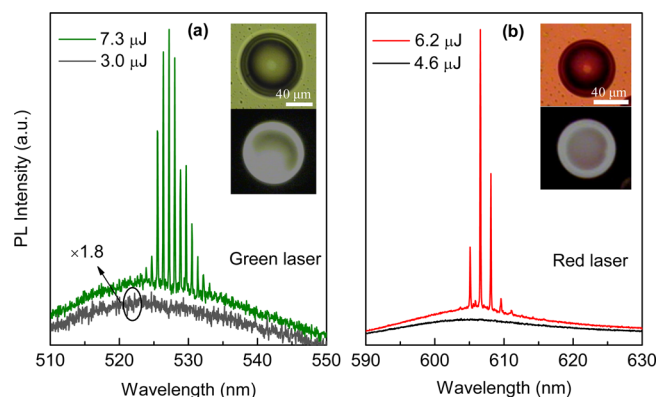


FIG. 3. (a) and (b) Spontaneous and laser emission from C540A and RhB doped cavities under optical pumping. FSR values of the hemispheres are 0.8 and 1.5 nm, respectively. The insets show optical and PL images of the corresponding hemispheres.

resonant wavelength, D is the diameter, and n_e is the effective refractive index of the hemisphere. Assuming, $n_e = 1.41$ and $D = 56.69 \mu\text{m}$, then the lasing peaks shown in Fig. 3(b) are well fitted with $m = 412\text{--}415$. Furthermore, FSR values of the hemispheres shown in Figs. 3(a) and 3(b) are ~ 0.8 and 1.5 nm, respectively. They are close to 0.75 and 1.48 nm, predicted by $\Delta\lambda = \lambda_m^2/\pi n_e D$.

To investigate energy transfer process, steady-state PL measurements of pure donor (C540A) and mixture of D-A (C540A-RhB) were performed. Figure 4 shows the normalized PL spectra of pure donor (normalized at the donor emission) and mixture D-A solutions (normalized at the acceptor emission). Stronger emission from the acceptor can be seen while the green emission decreased gradually as the concentration of acceptor increased. The peak intensity of donor emission decreases more than 20% when concentration of the acceptor is only about 3% compared with that of the donor. When the mole concentration of donor and acceptor are the same, the peak intensity of the green emission falls sharply to around 7% of its maximum, which indicates high energy transfer efficiency.

Figure 5 shows that multicolor lasing can be achieved from individual hemispheres with a certain D-A ratio doping. When the concentration of the acceptor is very low (D:A < 1:0.05), there were lasing modes at the green wavelength and spontaneous orange-red emission from the acceptor (Fig. 5(a)). The gain of the acceptor was not enough for lasing. In contrast, Fig. 5(b) shows that when the D:A ratio is about 1:0.1 or higher, strong acceptor lasing was observed while the emission from the donor was mostly suppressed. Interestingly, by investigating a number of hemispheres with similar sizes and the same concentration of acceptor doping, it is found that threshold of acceptor lasing (D:A is 1:1) was about 2.5 times lower than that of the pure acceptor lasing, which was attributed to the FRET from donor to acceptor (will be discussed later). Multicolor lasing with wavelength of 515–535 nm (green) and 585–605 nm (orange-red) were achieved from both donor and acceptor when D:A is around 1:0.07. For this ratio, proportion of energy from the donor was transferred to the acceptor, contributing to the observation of acceptor lasing, but this energy loss was insufficient to prevent the donor lasing.

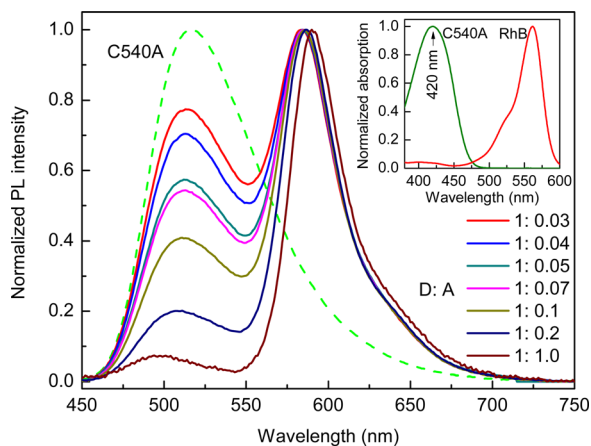


FIG. 4. Normalized PL spectra of pure donor and mixed donor-acceptor dye solutions with various ratios illuminated by Xe lamp at wavelength of 420 nm. The inset depicts the absorption spectra of the donor and acceptor.

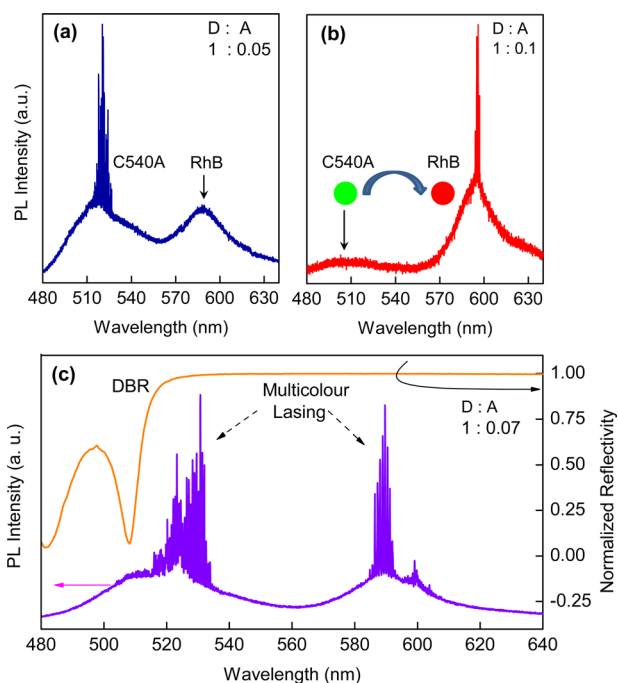


FIG. 5. Lasing spectra from individual hemispheres with various donor-acceptor ratios. (a) Donor lasing, (b) FRET-induced acceptor lasing, and (c) dual-colour donor and acceptor laser emission. Stop-band of the DBR used is shown in the top, which completely covers the lasing wavelength range.

The energy transfer process plays an important role in the observation of multicolor lasing. However, energy transfer can be either radiative or FRET.³⁰ To distinguish the two mechanisms, time resolved-PL measurements were carried for the pure donor and several D-A solutions. These samples were excited by a wavelength-tunable femtosecond laser with a wavelength of 420 nm, pulse duration of 100 fs, and a repetition rate of 1 kHz. The PL from the solutions were recorded by an Optronics streak camera with a temporal resolution of about 50 ps. Figure 6 plots fluorescence decays of pure donor and mixture of D-A with various ratios, detected at around 520 nm. The curves can be well fitted by

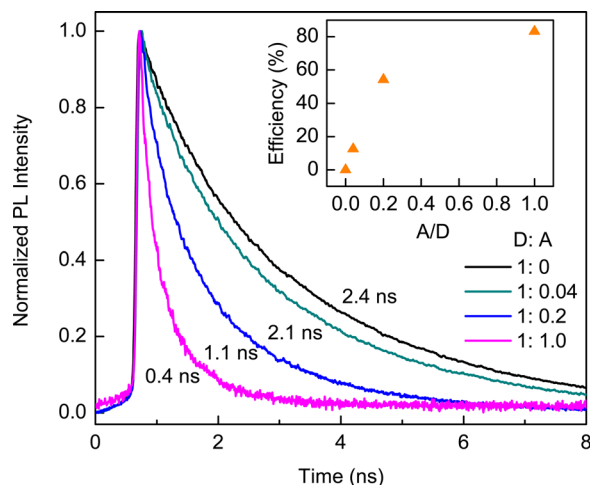


FIG. 6. Fluorescence decay curves of pure donor and donor-acceptor mixtures with various ratios detected at around 520 nm. Extracted lifetimes are shown on each curve. The inset presents energy transfer efficiency as a function of the acceptor:donor ratios.

an exponential decay function and the lifetime is extracted and given here. It can be seen clearly that the donor lifetime sharply falls with the increasing concentration of the acceptor. Pure donor has the longest lifetime of about 2.4 ns and decreases to 2.1 ns when concentration of the acceptor is only 4% of the donor. When number of acceptors is the same with that of donors, the lifetime of donor shows a significant drop to 0.4 ns.

The efficiency of FRET (η_e) can be estimated from the lifetime as $\eta_e = 1 - \tau/\tau_0$, where τ_0 and τ are lifetimes of pure donor and mixture D-A, respectively.³⁰ The inset of Fig. 6 depicts the efficiency of Förster transfer as a function of the A-D ratio, indicating an increase in the energy transfer efficiency from 12.5% to 83.3% for A-D of 0.04 and 1, respectively. This trend is understandable because the D-A separation distance decreases with an increase of acceptor concentration, which leads to the rise of energy transfer rate. As the efficiency of Förster transfer grows higher, FRET plays a more significant role in the acceptor lasing and offers lower lasing thresholds. As a result, FRET-induced lasing may be potential in high-efficiency lighting and display applications.

In summary, it has been demonstrated that inkjet printing is a highly suitable technique for mass production of high cavity Q-factor hemispherical microcavities (with the resulting Q-factors of the lasing modes $\sim 5 \times 10^3$). By embedding lasing dye mixtures into these structures, optically pumped lasers with emission at green (515–535 nm) and orange-red (585–605 nm) spectral ranges were achieved. The nonradiative FRET was the dominant effect with energy transfer efficiency up to 80%. Consequently, the acceptor lasing in presence of the donor featured a lower (~ 2.5 fold) threshold compared with the pure acceptor in the absence of donor. It is expected that the emission range of FRET-induced acceptor laser can be further expanded by cascading energy transfer processes through incorporating three or more dyes into the cavities.²⁸ White light laser is also possible by adding blue emission, which is significant for lighting and display technology.^{20,25}

This work was supported by the Singapore National Research Foundation through the Competitive Research Programme (CRP) under Project No. NRFCRP6-2010-02, the Singapore Ministry of Education through the Academic

Research Fund under Project Nos. MOE 2011-T3-1-005 (Tier 3) and Tier 1- RG92/15, and Merlion under Project No. 2.02.13.

- ¹K. J. Vahala, *Nature* **424**, 839 (2003).
- ²J. P. Reithmaier, G. Sek, A. Löffler, C. Hofmann, S. Kuhn, S. Reitzenstein, L. V. Keldysh, V. D. Kulakovskii, T. L. Reinecke, and A. Forchel, *Nature* **432**, 197 (2004).
- ³D. Englund, A. Faraon, I. Fushman, N. Stoltz, P. Petroff, and J. Vuckovic, *Nature* **450**, 857 (2007).
- ⁴Z. Li, Z. Zhang, A. Scherer, and D. Psaltis, *Opt. Express* **14**, 10494 (2006).
- ⁵J. Ward and O. Benson, *Laser Photonics Rev.* **5**, 553 (2011).
- ⁶F. Vollmer and S. Arnold, *Nat. Methods* **5**, 591 (2008).
- ⁷E. Verhagen, S. Deleglise, S. Weis, A. Schliesser, and T. J. Kippenberg, *Nature* **482**, 63 (2012).
- ⁸L. He, Ş. K. Özdemir, and L. Yang, *Laser Photonics Rev.* **7**, 60 (2013).
- ⁹V. D. Ta, R. Chen, L. Ma, Y. J. Ying, and H. D. Sun, *Laser Photonics Rev.* **7**, 133 (2013).
- ¹⁰Y. Wang, K. S. Leck, V. D. Ta, R. Chen, V. Nalla, Y. Gao, T. He, H. V. Demir, and H. Sun, *Adv. Mater.* **27**, 169 (2015).
- ¹¹M. Humar, M. Ravnik, S. Pajk, and I. Muševič, *Nat. Photonics* **3**, 595 (2009).
- ¹²V. D. Ta, R. Chen, and H. D. Sun, *Sci. Rep.* **3**, 1362 (2013).
- ¹³V. D. Ta, R. Chen, and H. D. Sun, *Adv. Mater.* **24**, OP60 (2012).
- ¹⁴S. K. Y. Tang, Z. Li, A. R. Abate, J. J. Agresti, D. A. Weitz, D. Psaltis, and G. M. Whitesides, *Lab Chip* **9**, 2767 (2009).
- ¹⁵V. D. Ta, R. Chen, D. M. Nguyen, and H. D. Sun, *Appl. Phys. Lett.* **102**, 031107 (2013).
- ¹⁶X. Fan and S.-H. Yun, *Nat. Methods* **11**, 141 (2014).
- ¹⁷S.-Y. Teh, R. Lin, L.-H. Hung, and A. P. Lee, *Lab Chip* **8**, 198 (2008).
- ¹⁸J. Lee, D. H. Kim, J.-Y. Kim, B. Yoo, J. W. Chung, J.-I. Park, B.-L. Lee, J. Y. Jung, J. S. Park, B. Koo, S. Im, J. W. Kim, B. Song, M.-H. Jung, J. E. Jang, Y. W. Jin, and S.-Y. Lee, *Adv. Mater.* **25**, 5886 (2013).
- ¹⁹M. Saito and K. Koyama, *Jpn. J. Appl. Phys., Part 1* **49**, 092501 (2010).
- ²⁰D. J. Gardiner, W. K. Hsiao, S. M. Morris, P. J. W. Hands, T. D. Wilkinson, I. M. Hutchings, and H. J. Coles, *Soft Matter* **8**, 9977 (2012).
- ²¹J. Haase, S. Shinohara, P. Mundra, G. Risse, V. G. Lyssenko, H. Frob, M. Hentschel, A. Eychmuller, and K. Leo, *Appl. Phys. Lett.* **97**, 211101 (2010).
- ²²A. J. C. Kuehne, M. C. Gather, I. A. Eydelnant, S.-H. Yun, D. A. Weitz, and A. R. Wheeler, *Lab Chip* **11**, 3716 (2011).
- ²³G. Aubry, Q. Kou, J. Soto-Velasco, C. Wang, S. Meance, J. J. He, and A. M. Haghiri-Gosnet, *Appl. Phys. Lett.* **98**, 111111 (2011).
- ²⁴C. Dang, J. Lee, C. Breen, J. S. Steckel, S. Coe-Sullivan, and A. Nurmikko, *Nat. Nanotechnol.* **7**, 335 (2012).
- ²⁵F. Fan, S. Turkdogan, Z. Liu, D. Shelhammer, and C. Z. Ning, *Nat. Nanotechnol.* **10**, 796 (2015).
- ²⁶T. Forster, *Discuss. Faraday Soc.* **27**, 7 (1959).
- ²⁷M. Berggren, A. Dodabalapur, R. E. Slusher, and Z. Bao, *Nature* **389**, 466 (1997).
- ²⁸S. I. Shopova, J. M. Cupps, P. Zhang, E. P. Henderson, S. Lacey, and X. Fan, *Opt. Express* **15**, 12735 (2007).
- ²⁹Y. Sun, S. I. Shopova, C.-S. Wu, S. Arnold, and X. Fan, *Proc. Natl. Acad. Sci. U.S.A.* **107**, 16039 (2010).
- ³⁰R. Chen, V. D. Ta, F. Xiao, Q. Zhang, and H. Sun, *Small* **9**, 1052 (2013).